THE UNIVERSITY OF MICHIGAN

COLLEGE OF ENGINEERING

DEPARTMENT OF ELECTRICAL ENGINEERING

Radiation Laboratory

VOR PARASITIC LOOP COUNTERPOISE - II :

INTERIM REPORT NO. 6

1 November 1970 - 31 January 1971

By

Dipak L. Sengupta and Joseph E. Ferris

26 February 1971

Contract FA69-WA-2085, Project 330-001-03N

Contract Monitor: Mr. Sterling R. Anderson

Prepared for

Federal Aviation Administration
Radar and Navaids Section
800 Independence Avenue, S.W.
Washington, DC 20590

Ann Arbor, Michigan

I INTRODUCTION

This is the Sixth Interim Report on Contract FA69-WA-2085, Project No., 330-001-03N, "VOR Parasitic Loop Counterpoise Systems-II," and covers the period 1 November 1970 to 31 January 1971.

During this period the full scale parasitic loop counterpoise antenna has been tested at the Manheim Road VOR Facility. Some of the results obtained so far are discussed in this report.

The following theoretical and numerical studies have also been carried out during this period in order to analyze the experimental results obtained:

(i) the variation of the field strength produced by the antenna at a distance of 300 feet away from the antenna,

(ii) the far field pattern of the antenna taking into account the effect of an ideal planar ground.

The results of the theoretical investigation are directly applicable to the analysis of the data obtained from the full scale testing of the parasitic loop counterpoise antenna at NAFEC (National Aviation Facility Experimental Center). At NAFEC the VOR parasitic loop counterpoise antenna is located at a height of 75 feet above the ground. The antenna system is excited at a frequency of 109 MHz (λ = 9.028 feet). The field produced by the antenna is detected by a horizontal dipole mounted on a vertical pole located at a distance of 300 feet away from the antenna. The detector height can be varied from the ground level to about 85 feet above the ground in steps of five feet.

II THEORETICAL ANALYSIS

In view of the fact that during the full scale testing, the direct and the reflected rays reaching the detector are not parallel to each other, it is clear that the detector is located in the quasi-radiation zone of the antenna. For this reason the analysis reported here is at first carried out for the case when the field point lies in the quasi-radiation zone so that the results can be compared directly with those obtained from the full scale test. We also discuss the case when the field point lies

in the conventional radiation zone. These results would be useful later for the analysis of flight test data.

2.1 Quasi-Radiation Zone Analysis

In this zone the usual geometrical optics approximation will be used. We consider the arrangement sketched in Figure 1 along with the coordinate system used. Let the field point P be located below the xy plane at (R, θ) from the origin of the coordinate system. The distance of the point P from the center of the antenna is D. It is evident from Figure 1 that the field at P would consist of the contributions from a direct and a reflected ray originating from the antenna.

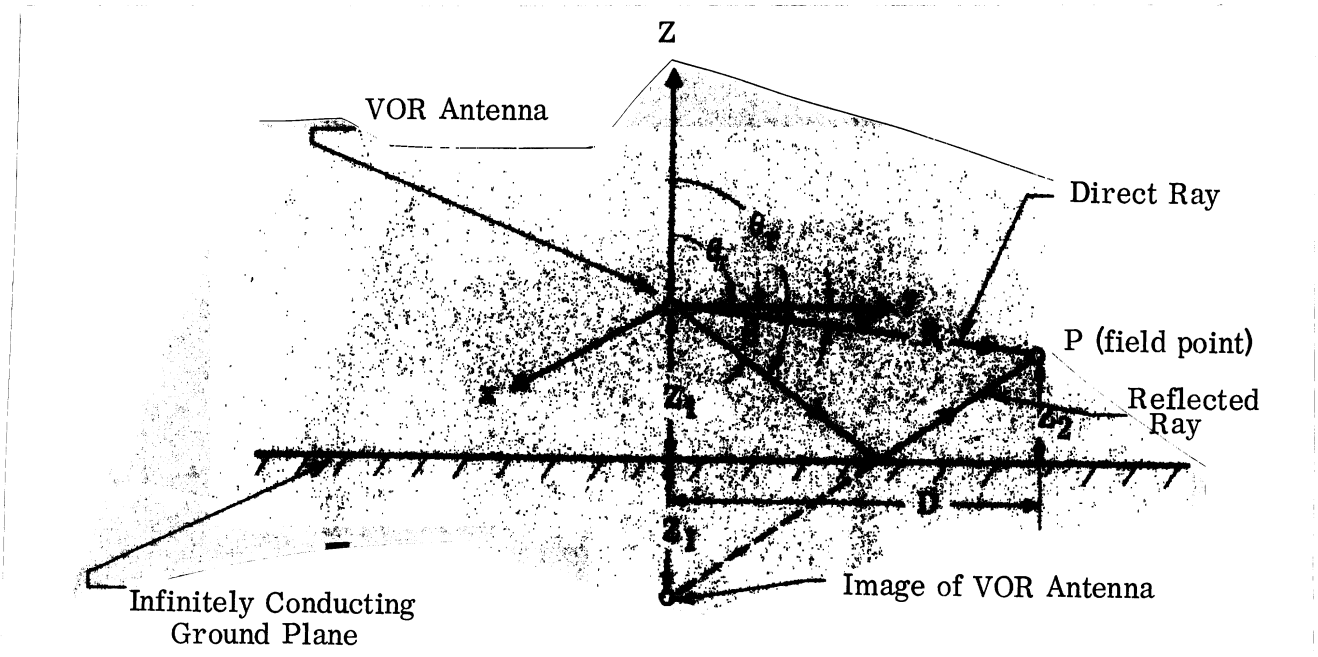

FIGURE 1: Geometrical representation of a non-uniformly excited double parasitic loop counterpoise antenna.

Let the free space electric field of the VOR antenna at a point (R, θ) in the radiation zone be given by the following expression:

$$\bar{E} = K \frac{e^{ikR}}{R} S(\theta) \hat{a}_{\phi} \quad , \tag{1}$$

where

$S(\theta)$ is the free space complex far field pattern of the antenna,
$\hat{a}_{\phi}$ is the unit vector in the ϕ-direction,
$k = 2\pi/\lambda$ is the free space propagation constant,
R, θ are the coordinates of the field point in spherical system,
and K is a constant.

Note that the field is polarized in the ϕ-direction, i.e. horizontally polarized.

In the present case, it is quite simple to show that the direct and reflected components of the electric field at the point P are given by

$$\bar{E}_D = K \cdot \frac{e^{ikR}}{R} S(\theta) \hat{a}_{\phi} \quad , \tag{2}$$

$$\bar{E}_r = -K \cdot \frac{e^{ikR'}}{R'} S(\theta_r) \hat{a}_{\phi} \quad , \tag{3}$$

where R' is the path length of the reflected ray between the source and field points and the other parameters are as shown in Figure 1. The negative sign in front of (3) appears because of the assumption of infinite conductivity for the ground. For a more realistic ground the negative sign in (3) should be replaced by a general reflection coefficient

$$\Gamma = |\Gamma| e^{j\delta} \quad .$$

From Figure 1 it can be shown that

$$\theta = \frac{\pi}{2} + \alpha \quad , \qquad \theta_r = \frac{\pi}{2} + \beta \tag{4}$$

and

$$\tan\alpha = \frac{Z_1 - Z_2}{D} \quad , \quad \tan\beta = \frac{Z_1 + Z_2}{D} \quad . \tag{5}$$

It can also be seen from Figure 1 that

$$R^2 = D^2 + (Z_1 - Z_2)^2 \quad , \quad R'^2 = D^2 + (Z_1 + Z_2) \quad . \tag{6}$$

Assuming Z_1, $Z_2 << D$ it can be shown that

$$R' \simeq R + \frac{2Z_1 Z_2}{D} \quad . \tag{7}$$

Using Eqs. (2), (3) and (7) it can be shown that the total field $\bar{E}_T$ at P is given by

$$\bar{E}_T = \bar{E}_D + \bar{E}_r \simeq K \cdot \frac{e^{ikR}}{R} \left[S(\theta) - e^{ik\frac{2Z_1 Z_2}{D}} S(\theta_r) \right] \hat{a}_\phi \quad . \tag{8}$$

Thus the complex field pattern $S_T(\theta)$ produced by the antenna configuration shown in Figure 1 can be written as

$$S_T(\theta) = S'(\theta) - S(\theta_r) e^{ik\frac{2Z_1 Z_2}{D}} \tag{9}$$

where θ and θ_r are given by Eqs. (4) and (5).

If the field point P is taken to be above the xy plane, then the complex field pattern is again given by (9) but with the following modified definitions of θ and θ_r.

$$\tan\theta = \frac{D}{Z_2 - Z_1} \quad , \quad \theta_r = \frac{\pi}{2} + \beta, \quad \tan\beta = \frac{Z_1 + Z_2}{D} \quad . \tag{10}$$

2.2 Numerical Results

As mentioned before, $S(\theta)$ represents the free space complex far field pattern produced by the VOR antenna under consideration. For the present case, the antenna is taken to be the non-uniformly excited double parasitic loop counterpoise antenna. For such an antenna, explicit expressions for $S(\theta)$ have been derived and discussed (Interim Report 3051-3-T, May 1970) and hence will not be repeated here. The basic physical parameters of the antenna are as shown in Figure 2.

Equation (9) has been computed for $kZ_1 = 52.20$, $kD = 208.80$ and kZ_2 varying from 0 to 72.95. These values correspond to $Z_1 = 75'$, $D = 300'$ and Z_2 varying from 0 to 105' which are being used for the full scale testing at 109 MHz at NAFEC. For the above values of Z_1, Z_2 and D the patterns have been computed in the region of space above and below the horizon, for different combinations of the parameters B_1, B_2, H_1 and H_2.

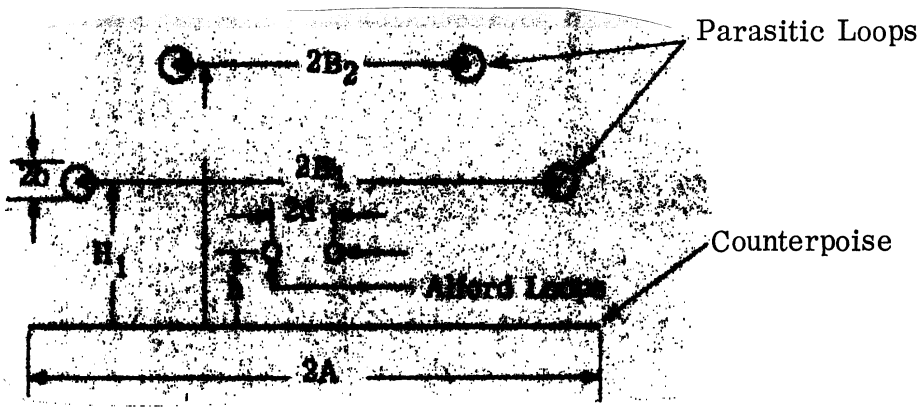

FIGURE 2: Geometrical representation of the VOR Antenna above a perfectly conducting infinite planar ground.

Figures 3, 4 and 5 give the theoretical $|S_T(\theta)|$ versus θ for some typical selected cases. The corresponding free space values are also shown on these curves so that the effects of ground reflection may be directly ascertained. The free space values shown in Figures 3 through 5 will have some error due to the fact that it is assumed the field points are at a constant distance from the antenna (see Eq. 4) . However, since Z_1, $Z_2 << D$ this error would be very small.

Figure 3 is for the case when the double parasitic loop counterpoise antenna is designed (on the free space basis) to produce maximum field gradient at the horizon at the frequency of 109 MHz. The effects of the ground reflection on the pattern is obvious from Figure 3. The lobings in the pattern are attributed to the reflection effects. The field gradient in the free space pattern is about 23.7 dB/6°; from Figure 3 it can be seen that in the presence of ground reflection the average field gradient from the same antenna is about 16.6 dB/6°. In addition to this, the reflection effects develop minor lobes in the pattern region where it was designed to have a null.

Figure 4 gives similar results for an antenna designed to have optimum performance at 108 MHz.

Figure 5 gives the results obtained from the same antennas as that of Figure 4 but operated at the frequency of 109 MHz.

Figures 6, 7 and 8 give the theoretical $|S_T(\theta)|$ vs θ for some typical selected parasitic loop counterpoise antennas when the antennas are excited omnidirectionally. The general nature of these curves with and without ground reflection effects are similar to those in Figures 3, 4 and 5. In comparison with the previous cases, however, it is found that the variation of field with θ, at a distance 300 feet away from the antenna, is less pronounced. This is evident from the weak lobings in the patterns. This may be attributed to the fact that in the omnidirectional case, the free space field varies much more slowly below the horizon.

In Figure 6, we have shown the corresponding points obtained from the full scale test results. The agreement between them and experiment is found to be very good.

2.3 Radiation Zone Analysis

In this zone the field point is located at an infinite distance from the antenna so that the direct and reflected rays reaching the field point may be assumed to be parallel to each other. Under this condition it can be shown that the far field pattern is given by the following expression:

$$S_T(\theta)=S(\theta)e^{-ikZ_1\cos\theta} - S(\pi-\theta)e^{ikZ_1\cos\theta}, \qquad (11)$$

for $0 < \theta < \pi/\sigma$. For $\theta = \pi/2$, $S_T(\theta) = 0$ which is consistent with the assumption of perfectly conducting planar ground with horizontally polarized incident field. Two of the typical patterns obtained by numerical computations of (11) are shown in Figures 9 and 10. Figure 9 uses the same antenna used in Figure 3 and Figure 10 uses the same antenna as in Figure 5. On Figure 9 the corresponding free space pattern points are marked x. It can be seen from Figure 9 that the two patterns are almost identical. In this case it is concluded that the pattern of the antenna in the range $0 < \theta < \pi/2$ is not appreciably affected by ground reflection. Similar comments apply to the results shown in Figure 10. Note that this is due to the fact that the antenna was originally designed to produce very low level fields in directions $\theta > \pi/2$. Of course, the field in the direction $\theta = \pi/2$ reduces to zero due to reflection.

III FULL SCALE TEST RESULTS

A typical experimental pattern obtained at NAFEC at 109 MHz is shown in Figure 11. The relevant parameters of the VOR parasitic loop counterpoise antenna used are $kB_1 = 16.18$, $kH_1 = 3.32$, $kB_2 = 11.31$ and $kH_2 = 13.34$ at 109 MHz. These parameters are very close to those used in Figure 5. The agreement between the initial regions of Figures 5 and 11 may be considered to be very good in view of the various approximations used in the analysis. We thus conclude that the full scale test results that are being obtained at present are in fair agreement with the theoretical predictions obtained from the numerical study. Further discussion of the test results will be given in a later report.

IV CONCLUSIONS

On the basis of the results discussed above it may be concluded that the full scale test results are in fair agreement with the numerical results obtained by computing theoretical expressions derived earlier. The agreement between the two may be further improved by assuming a more realistic reflection coefficient for the ground for the analysis reported. During the coming period tests will be conducted to ascertain the performance of the parasitic loop counterpoise antenna under actual flight conditions.

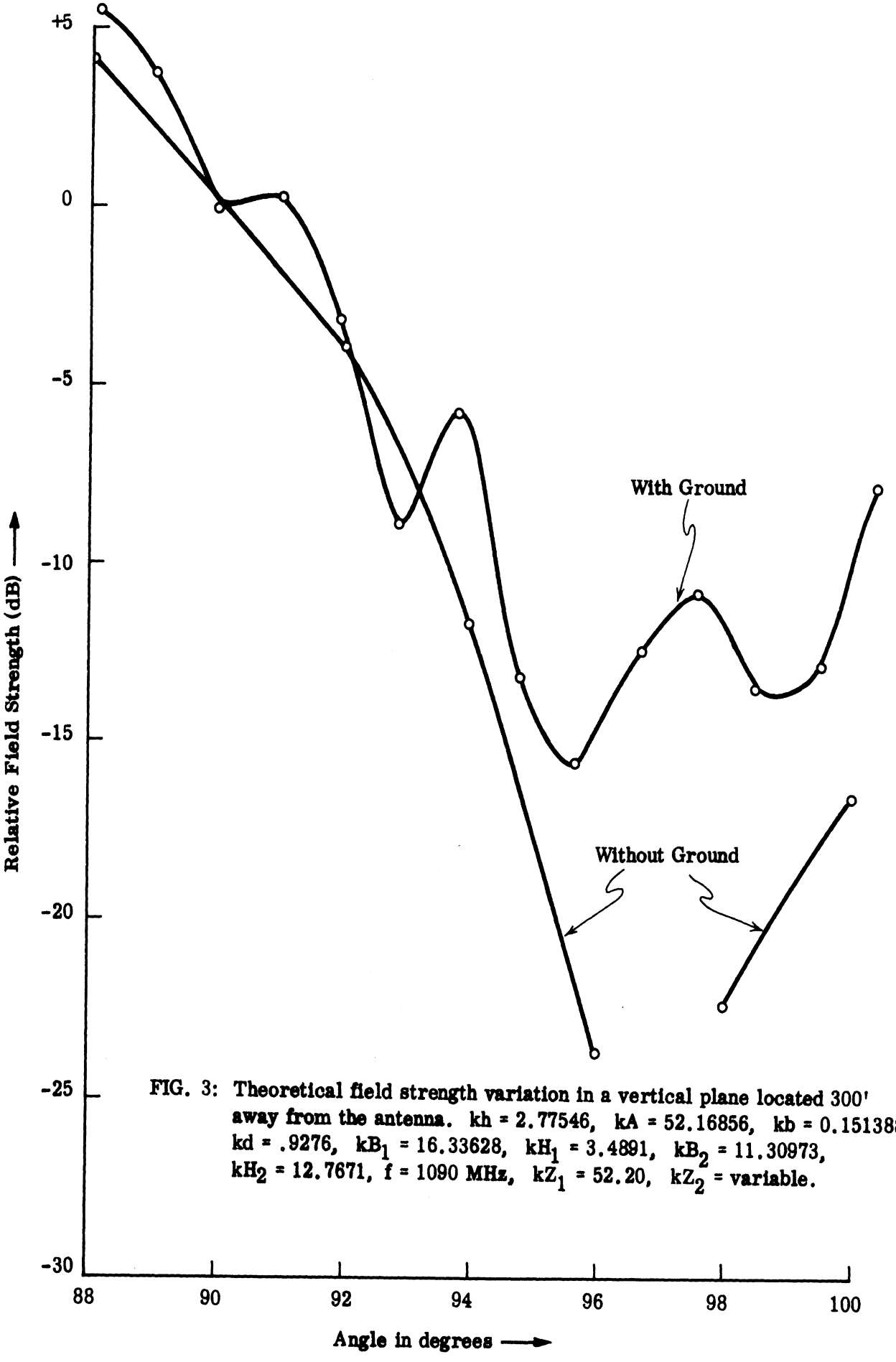

FIG. 3: Theoretical field strength variation in a vertical plane located 300' away from the antenna. kh = 2.77546, kA = 52.16856, kb = 0.1513887, kd = .9276, kB_1 = 16.33628, kH_1 = 3.4891, kB_2 = 11.30973, kH_2 = 12.7671, f = 1090 MHz, kZ_1 = 52.20, kZ_2 = variable.

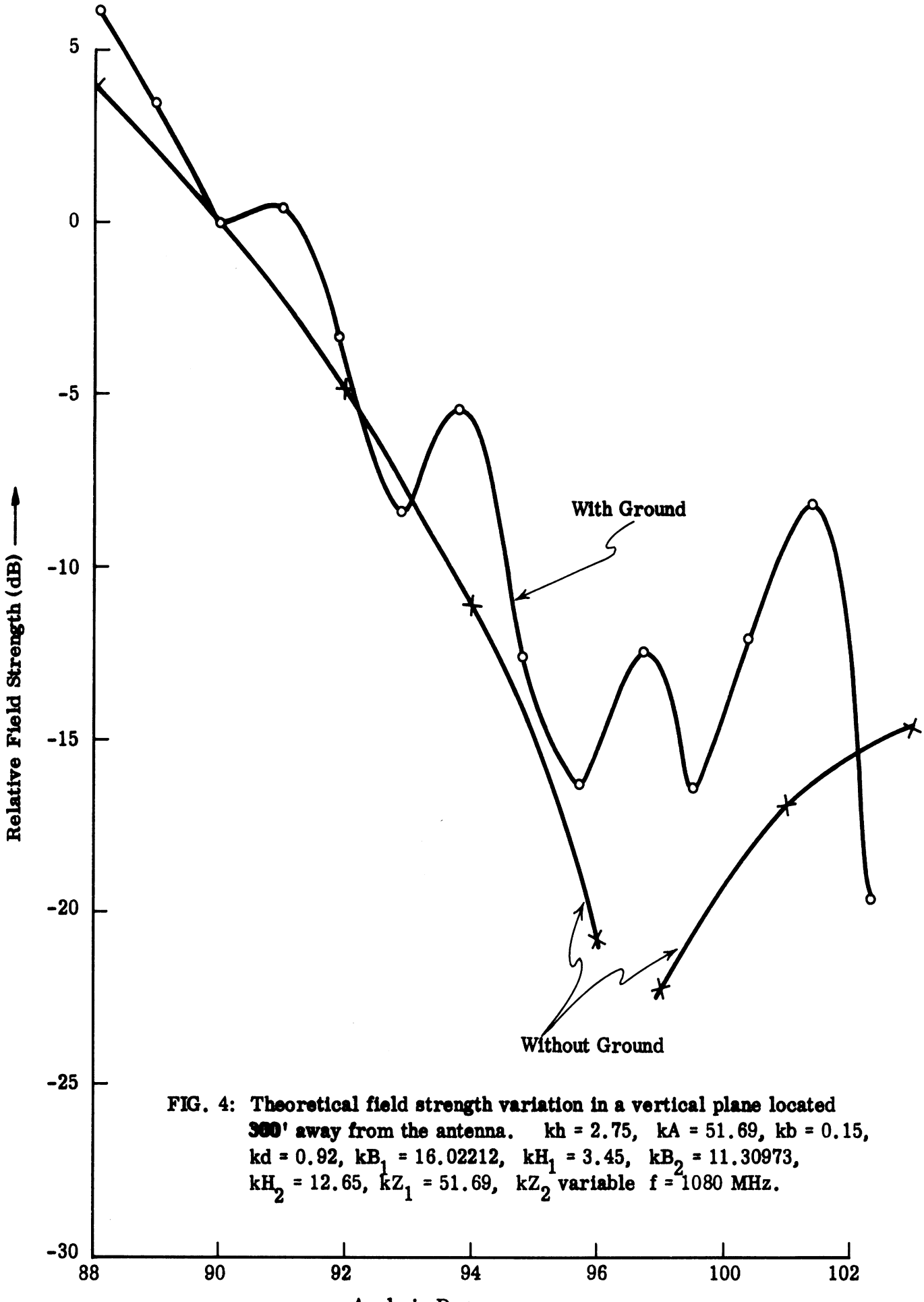

FIG. 4: Theoretical field strength variation in a vertical plane located 300' away from the antenna. kh = 2.75, kA = 51.69, kb = 0.15, kd = 0.92, kB_1 = 16.02212, kH_1 = 3.45, kB_2 = 11.30973, kH_2 = 12.65, kZ_1 = 51.69, kZ_2 variable f = 1080 MHz.

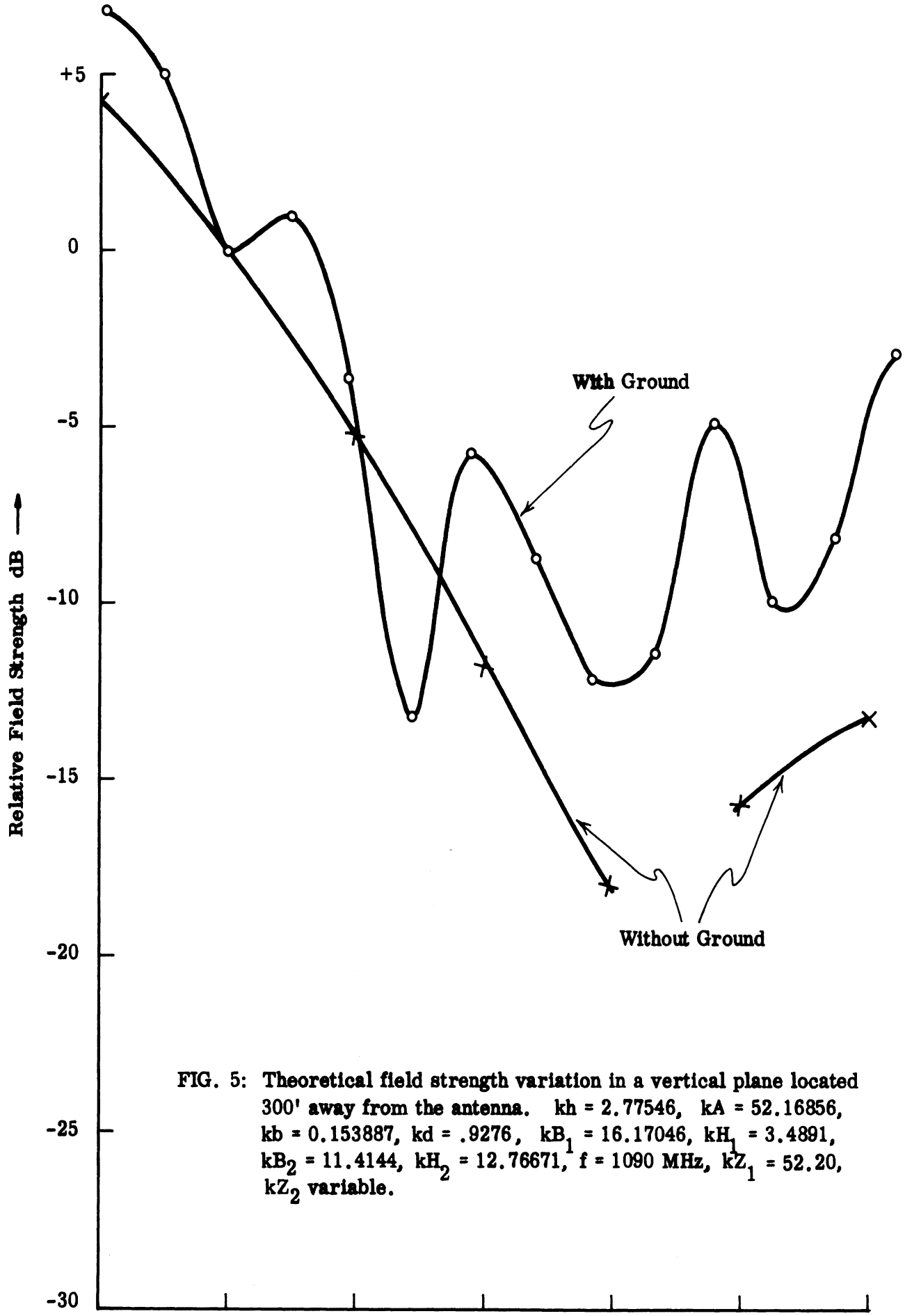

FIG. 5: Theoretical field strength variation in a vertical plane located 300' away from the antenna. kh = 2.77546, kA = 52.16856, kb = 0.153887, kd = .9276, kB_1 = 16.17046, kH_1 = 3.4891, kB_2 = 11.4144, kH_2 = 12.76671, f = 1090 MHz, kZ_1 = 52.20, kZ_2 variable.

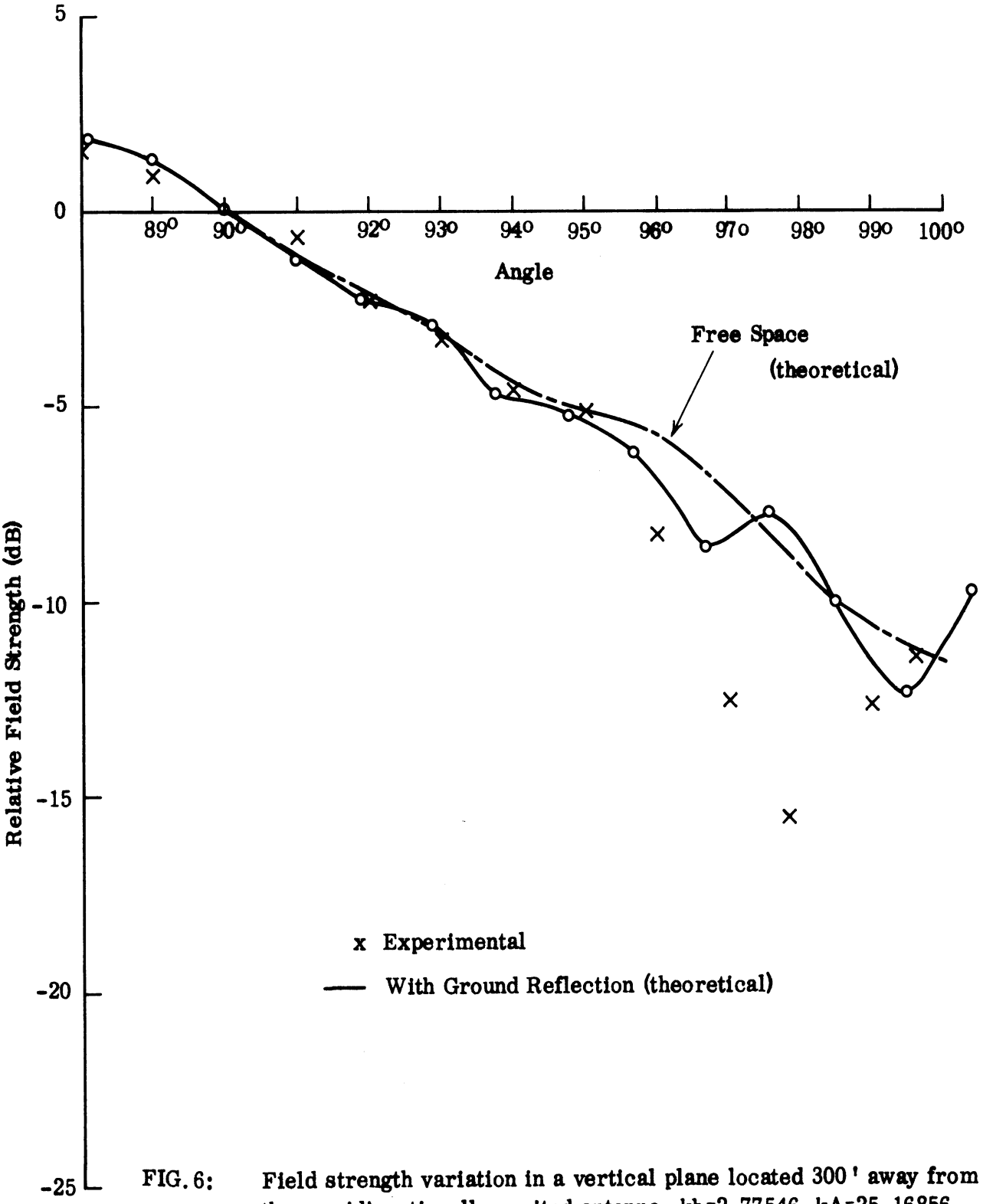

FIG. 6: Field strength variation in a vertical plane located 300' away from the omnidirectionally excited antenna. kh=2.77546, kA=25.16856, kb=0.1513887, kB_1=16.18, kH_1=3.32, kB_2= 11.31, kH_2=13.34, f= 109 MHz.

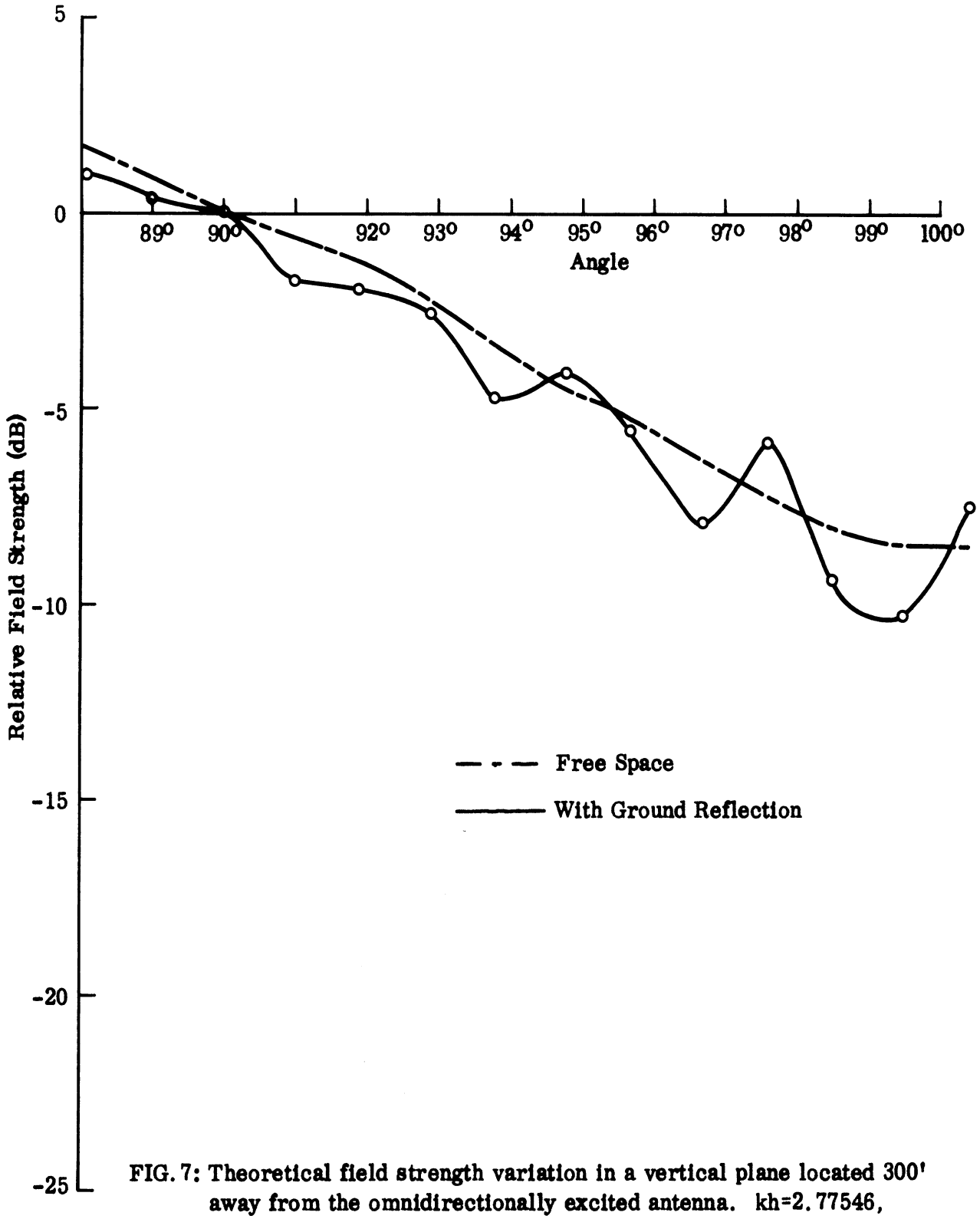

FIG. 7: Theoretical field strength variation in a vertical plane located 300' away from the omnidirectionally excited antenna. kh=2.77546, kA=52.16856, kb=0.1513887, kB_1=16.17, kH_1=3.4891, kB_2=11.414, kH_2=12.7671, f=109 MHz.

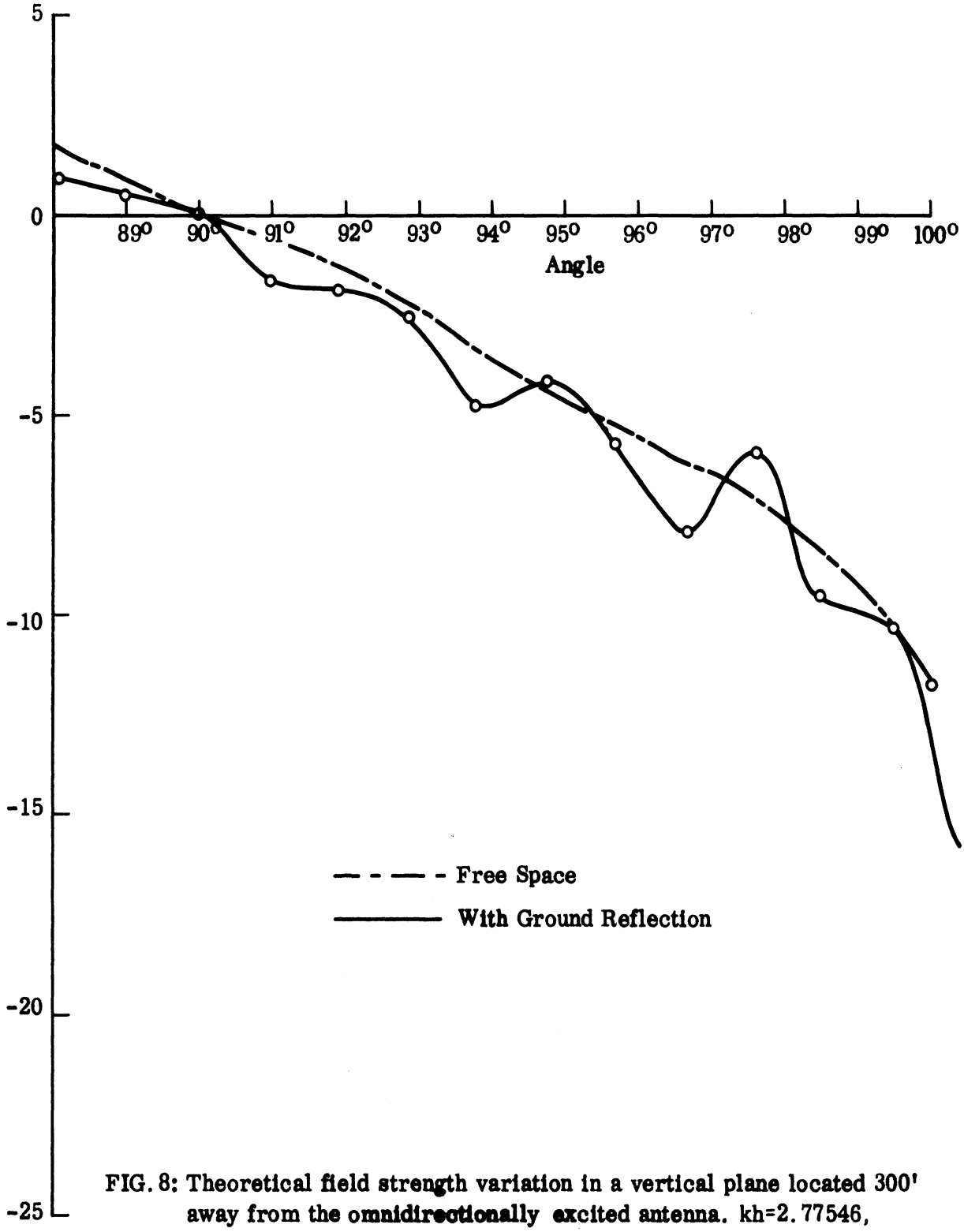

FIG. 8: Theoretical field strength variation in a vertical plane located 300' away from the omnidirectionally excited antenna. kh=2.77546, kA=52.16856, kb=0.1513887, kB_1=16.33628, kH_1=3.4891, kB_2=11.30973, kH_2=12.7671, f=109 MHz.

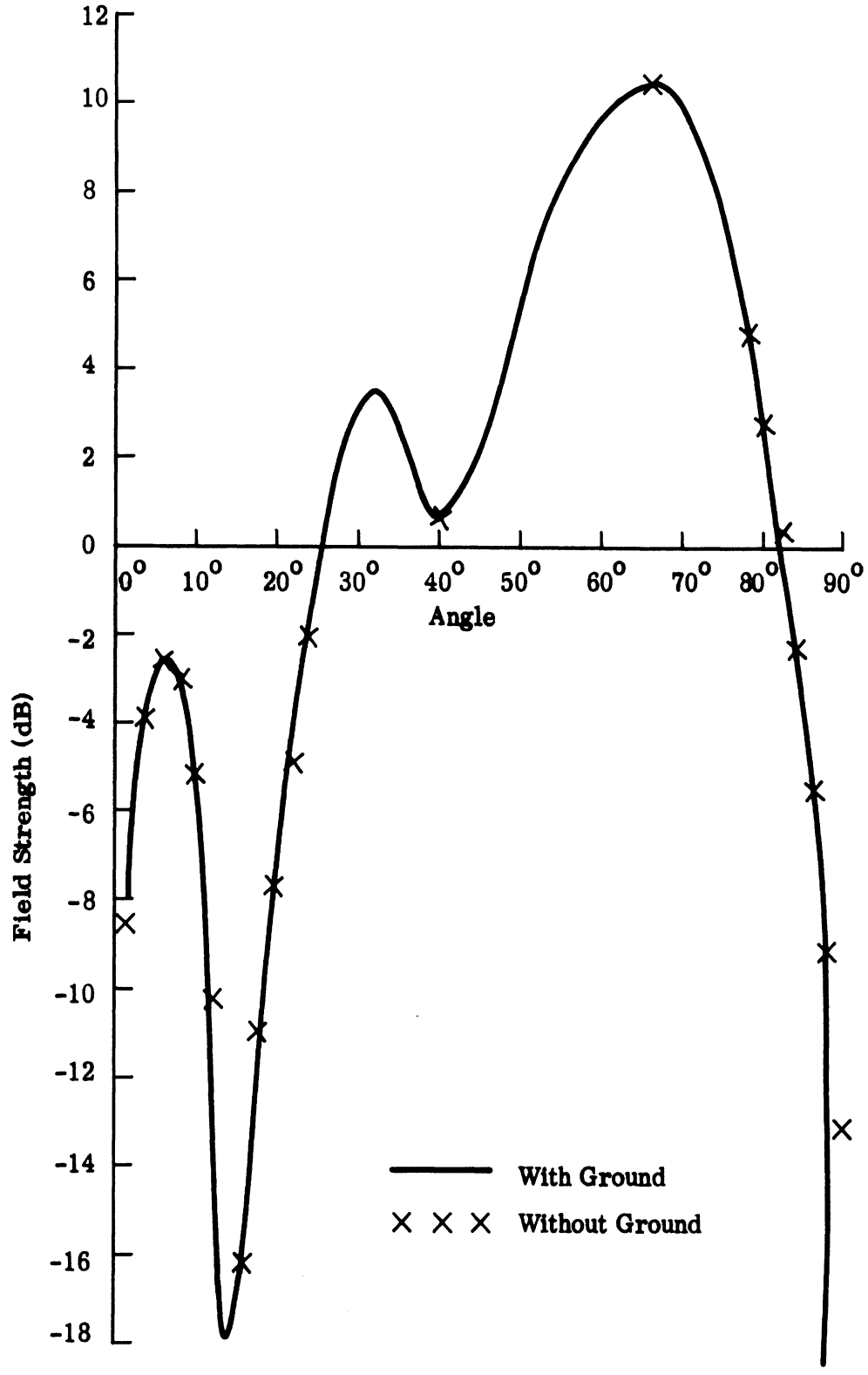

FIG. 9: Theoretical elevation radiation pattern of the antenna of Fig. 3 located above ground $kZ_1 = 52.20$, f = 109 MHz.

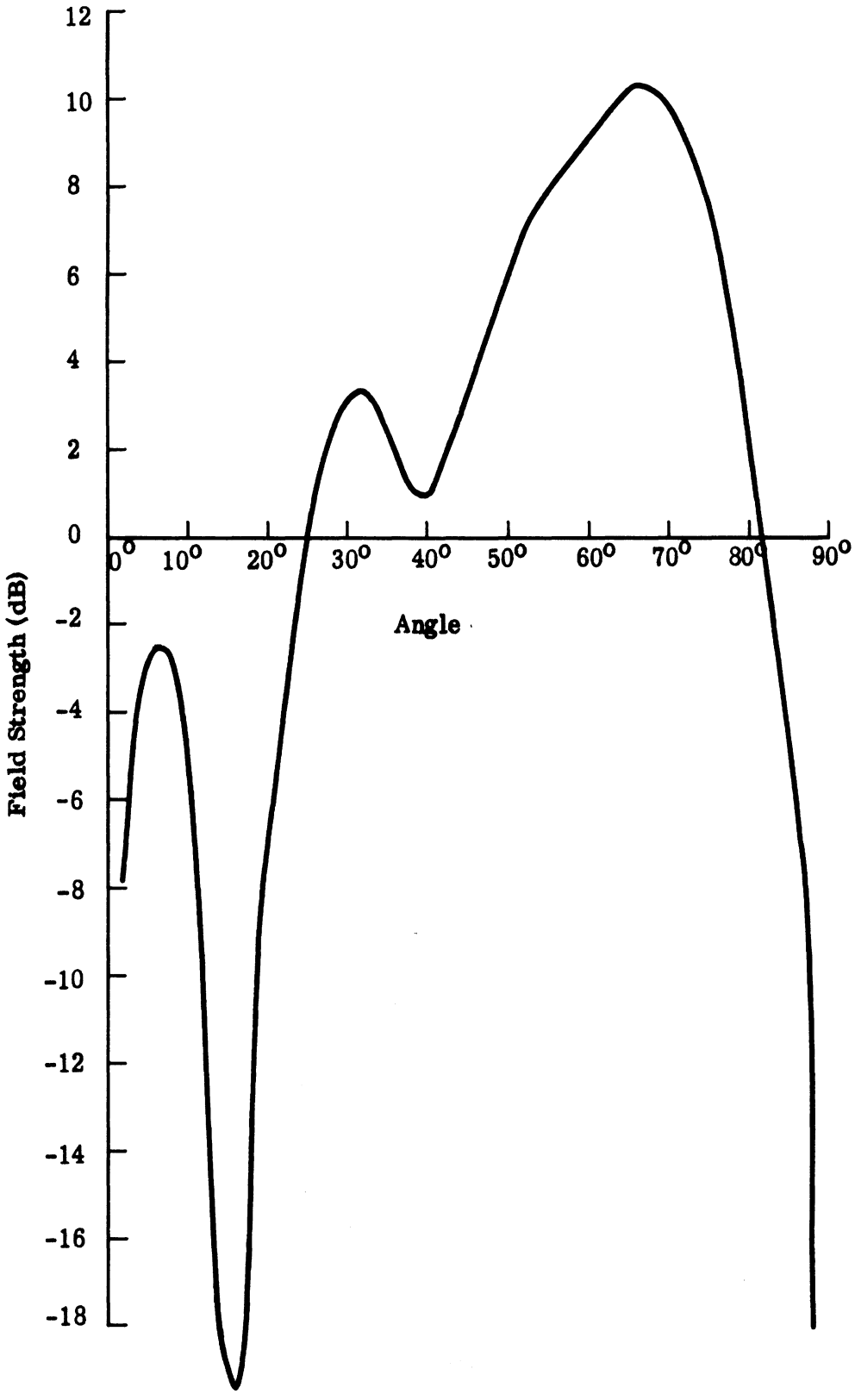

FIG. 10: Theoretical elevation radiation pattern of the antenna of Fig. 5 located above ground $kZ_1 = 52.20$, f = 109 MHz.

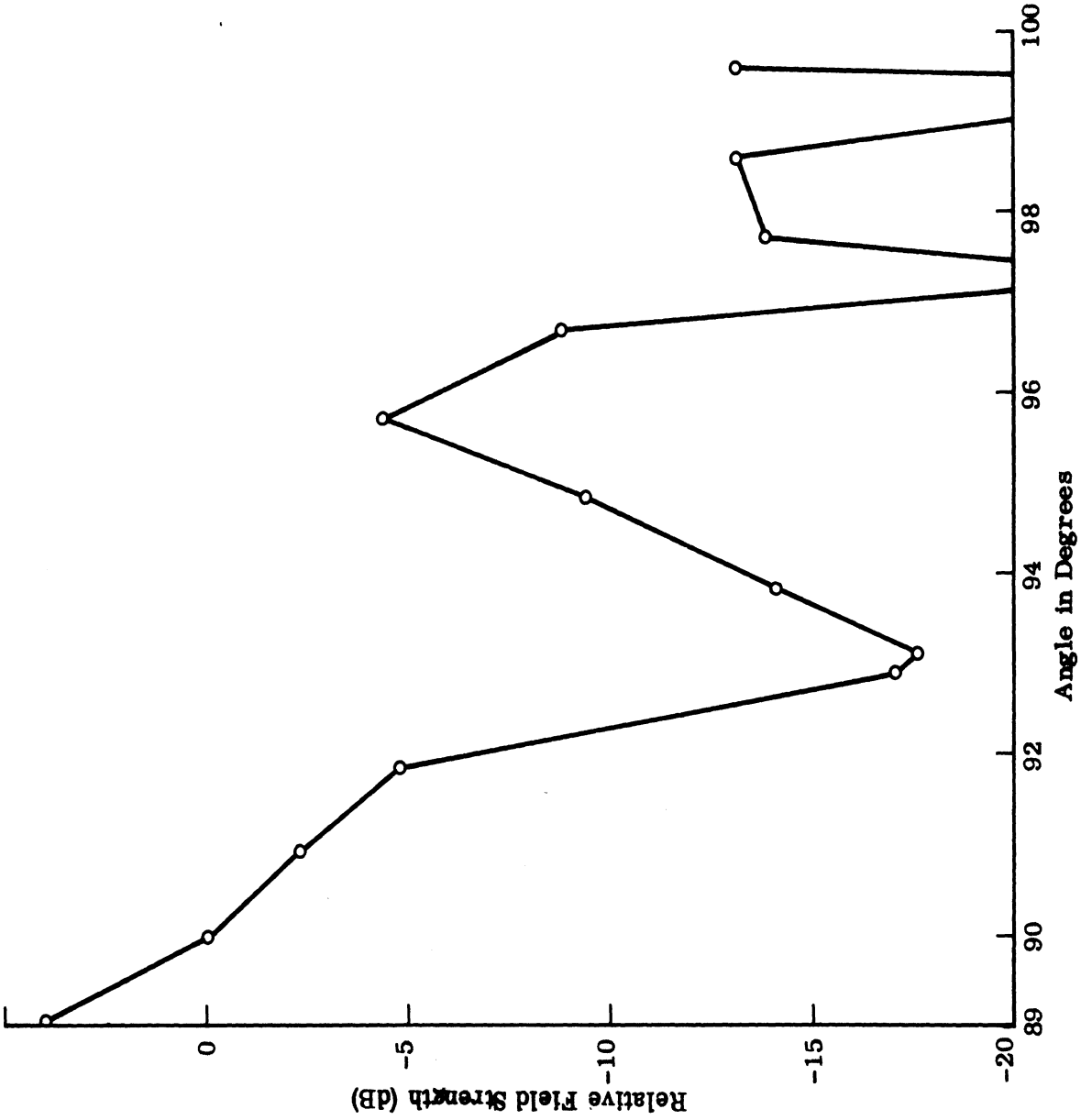

FIG. 11: Measured field strength variation in a vertical plane located 300' away from the antenna. kh=2.77546, kA=52.16856, kb=0.1513887, kd=0.9276, kB_1=16.18, kH_1=3.32, kB_2=11.31, kH_2=13.34, kZ_1=52.20, kZ_2 variable f= 109 MHz.